

8-5-2013

Frequency response of atmospheric pressure gas breakdown in micro/nanogaps

Abbas Semnani

Birck Nanotechnology Center, Purdue University, asemnani@purdue.edu

Ayyaswamy Venkatraman

Birck Nanotechnology Center, Purdue University, venkatt@purdue.edu

Alina A. Alexeenko

Birck Nanotechnology Center, Purdue University, alexeenk@purdue.edu

Dimitrios Peroulis

Birck Nanotechnology Center, Purdue University, dperouli@purdue.edu

Follow this and additional works at: <http://docs.lib.purdue.edu/nanopub>



Part of the [Nanoscience and Nanotechnology Commons](#)

Semnani, Abbas; Venkatraman, Ayyaswamy; Alexeenko, Alina A.; and Peroulis, Dimitrios, "Frequency response of atmospheric pressure gas breakdown in micro/nanogaps" (2013). *Birck and NCN Publications*. Paper 1445.
<http://dx.doi.org/10.1063/1.4817978>

This document has been made available through Purdue e-Pubs, a service of the Purdue University Libraries. Please contact epubs@purdue.edu for additional information.

Frequency response of atmospheric pressure gas breakdown in micro/nanogaps

Abbas Semnani, Ayyaswamy Venkatraman, Alina A. Alexeenko, and Dimitrios Peroulis

Citation: *Applied Physics Letters* **103**, 063102 (2013); doi: 10.1063/1.4817978

View online: <http://dx.doi.org/10.1063/1.4817978>

View Table of Contents: <http://scitation.aip.org/content/aip/journal/apl/103/6?ver=pdfcov>

Published by the [AIP Publishing](#)

Advertisement:



Goodfellow

metals • ceramics • polymers
composites • compounds • glasses

Save 5% • Buy online
70,000 products • Fast shipping

Frequency response of atmospheric pressure gas breakdown in micro/nanogaps

Abbas Semnani,^{1,a)} Ayyaswamy Venkatraman,² Alina A. Alexeenko,² and Dimitrios Peroulis¹

¹*School of Electrical and Computer Engineering, Birck Nanotechnology Center, Purdue University, West Lafayette, Indiana 47907, USA*

²*School of Aeronautics and Astronautics, Purdue University, West Lafayette, Indiana 47907, USA*

(Received 4 July 2013; accepted 24 July 2013; published online 6 August 2013)

In this paper, we study gas breakdown in micro/nanogaps at atmospheric pressure from low RF to high millimeter band. For gaps larger than about 10 μm , the breakdown voltage agrees with macroscale vacuum experiments, exhibiting a sharp decrease at a critical frequency, due to transition between the boundary- and diffusion-controlled regimes, and a gradual increase at very high frequencies as a result of inefficient energy transfer by field. For sub-micron gaps, a much lower breakdown is obtained almost independent of frequency because of the dominance of field emission. © 2013 AIP Publishing LLC. [<http://dx.doi.org/10.1063/1.4817978>]

Gas breakdown in AC fields is not well understood for micro/nanogaps especially in GHz to THz frequency range. In such gaps, breakdown could occur at relatively low voltages which may generate electric fields in the order of tens of $\text{V}/\mu\text{m}$.¹ While achieving gas breakdown is desirable in several applications that involve microplasma generation,^{2,3} it can lead to performance degradation and failure in micro and nanoelectronic devices and circuits.^{4,5} It has been well established that gas discharges at all length scales are driven by an interplay of three major mechanisms of electron-impact ionization (EII), secondary electron emission (SEE), and field emission (FE).¹ In gaps $>7 \mu\text{m}$, it has been shown that EII and SEE are the key mechanisms responsible for breakdown and the physics is accurately captured by the traditional Paschen curve.¹ It was also established later⁶ that FE due to electron tunneling at the cathode becomes the dominant mechanism for smaller gaps^{7,8} resulting in various modified Paschen curves and other scaling laws that capture all the relevant physics in the entire range of gap sizes.^{9,10}

The DC^{11,12} and low RF breakdown^{13–15} have been addressed extensively through theory, simulations, and measurements. In contrast, gas breakdown due to high frequency time-varying fields especially in micro/nanogaps^{16–18} remains poorly understood and has not been described by a general scaling law. The AC breakdown problem has been studied since 1950s.^{19,20} A few generalizations also exist for breakdown voltage as a function of frequency-gap $f \times d$ and pressure-gap $p \times d$ based on vacuum experiments. These breakdown relationships, however, do not apply when the same $p \times d$ values are obtained in GHz to THz gaps at atmospheric pressures when the excitation frequency becomes comparable with the particle collision frequency. While a few theories to calculate breakdown field in high frequencies exist in literature,^{21–23} these are highly restrictive when applied to micro/nanogaps. For example, AC air breakdown model introduced in Ref. 21, considers neither FE nor SEE effects that are important at nano/microgaps.²⁴

The main goal of this paper is to investigate the frequency response of breakdown voltage in atmospheric pressure micro/nanoscale gaps. We apply numerical plasma simulations to characterize the behavior of the breakdown voltage as a function of applied frequency. The results are used to define various regimes in the frequency domain, delineated by distinct driving mechanisms. An approach for finding a *critical frequency* as a function of gap size, gas and electrode properties is then formulated. The quantitative results provide a better understanding of high frequency micro and nanoscale gas breakdown useful for development of accurate high-frequency breakdown theories and evaluation of safe operating regimes for RF micro and nanoelectronics.

The breakdown process in gap lengths in the range of hundreds of nm to a few μm is modeled using the particle-in-cell with Monte Carlo collision (PIC/MCC) method.^{25,26} It is assumed that the dimensions of the electrodes are much larger than the gap size and the discharge is considered to be one-dimensional (1-D). This simplifying assumption allows a detailed analysis of the fundamental physics involved and is a valid assumption for a large number of micro and nanoplasma problems. The operating pressure for all cases was taken as 760 Torr and gas temperature of 300 K was assumed to be constant. In order to obtain the breakdown voltage (V_{bd}), the time evolution of electron number density is tracked. The V_{bd} value corresponds to the switch between decreasing to increasing behavior of the electron number density inside the gap. In order to minimize the total number of simulations, the V_{bd} value for a given frequency was obtained with about 2% uncertainty. The frequency range is considered from DC to hundreds of GHz to clearly distinguish the various regimes in the frequency domain with each regime controlled by a certain discharge mechanism.

Three included electron-neutral collisions are elastic scattering, electronic excitation, and ionization. The excited neutrals, however, are not tracked since it is assumed that their lifetimes are very short and do not modify the relevant physics, significantly. Two ion-neutral collisions including elastic scattering and charge exchange are considered. Also,

^{a)}Electronic mail: asemnani@purdue.edu

it is assumed that the magnetic field is negligible and Poisson's equation is solved instead of the full set of Maxwell's equations. The timestep varies between 10^{-17} and 10^{-15} s to satisfy the standard timestep restrictions for numerical convergence of PIC/MCC technique by considering also the cell sizes equal to 20 nm.²⁶

The plasma dynamics in DC discharges is relatively straightforward when compared to time-varying fields. In DC, charged particles are generated due to EII, SEE, and FE with electrons and ions drifting, respectively, towards the anode and cathode where they are absorbed at the walls. Recombination reactions also contribute to a small fraction of loss of charged species. When the generation rate becomes higher than the loss rate, charge accumulation in the gap eventually leads to DC breakdown. However when in RF cases, the polarities of the electrodes change every half cycle, the following three scenarios could occur depending on the gap length, gas composition, amplitude, and frequency of the applied field.

1. The frequency is sufficiently low such that a large fraction of electrons and ions reach and are lost to the electrodes each half cycle before the polarities are reversed.
2. The frequency is high enough such that the electrons with higher drift velocities are still lost to the walls but the ions are trapped in the gap since their drift velocity is significantly lower than the electrons.
3. The frequency is very high resulting in the trapping of both electrons and ions in the gap.

The first two scenarios are qualitatively similar to the dynamics in DC discharge. However in the third scenario, absorption by the walls is eliminated resulting in a rapid increase in the number of electrons which in turn participate in ionizing collisions to increase the number of ions. Under these conditions, gas breakdown occurs at a significantly lower voltage compared to the first two scenarios. It has been shown²⁷ that for a given gap length, d , electrons do not reach the boundaries if the applied frequency is larger than a critical frequency, f_{cr} , given by

$$f_{cr} = \frac{eV_{rms}}{\pi m \nu_c d^2}, \quad (1)$$

where e is the electron charge, V_{rms} represents the root mean square voltage, and m is the mass of the electrons. Also, ν_c is the electron-neutral collision frequency which is estimated by

$$\nu_c = C \times p, \quad (2)$$

where p is the pressure in Torr and C is a gas dependent parameter which is equal to 4.2×10^9 and 5.3×10^9 ($s^{-1} \text{Torr}^{-1}$) for nitrogen and argon, respectively.¹

In order to quantitatively demonstrate the influence of frequency on the breakdown voltage, simulations are performed for two different operating conditions. The first case is a 19 μm gap with nitrogen gas and copper electrodes with a work function, ϕ , of 4.7 eV. Field enhancement factor (β) due to surface roughness of electrodes was taken as 70, which is a typical value based on measurements performed using microstructures.²⁸ The SEE coefficient, γ_{se} , was set to 0.1 based on an empirical equation,¹

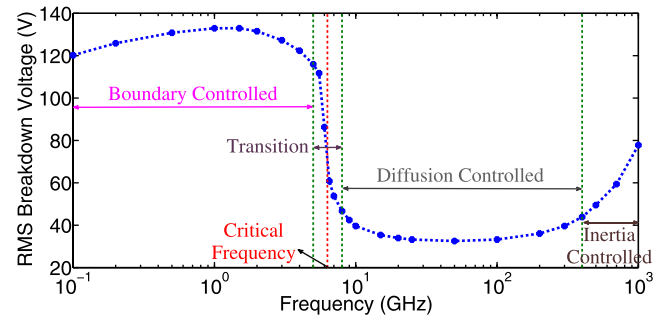


FIG. 1. Frequency response of breakdown voltage and the predicted critical frequency point in a 19 μm nitrogen gap with copper electrodes. $\phi = 4.7$ eV, $\beta = 70$, and $\gamma_{se} = 0.1$.

$$\gamma_{se} = 0.016 \times (IE - 2\phi), \quad (3)$$

where IE is the ionization energy of the gas in eV.

The frequency response of breakdown voltage for the nitrogen-copper case for frequencies ranging from 100 MHz to 1 THz is presented in Fig. 1. It is observed that for frequencies less than the critical frequency (6.3 GHz as reported in Table I), variation of the breakdown voltage is small (less than 10% up to 5 GHz). This frequency range corresponds to the first two scenarios where most of the electrons reach the electrodes thereby being lost resulting in similar effective breakdown voltages for both DC and RF fields. Since this region is characterized by frequencies lower than the critical frequency, it was referred as low frequency breakdown regime in some literature.²⁰ However, since it can continue up to tens of GHz for microgaps, we refer to this regime as the *boundary controlled regime* which implies that the breakdown is governed by boundary processes such as FE and SEE depending on the gap size. A small increase of breakdown voltage in this region is due to decrease in the number of ions that reach the cathode as frequency increases. This in turn decreases SEE which is the main driving mechanism for a 19 μm gap and hence increases V_{bd} .

For frequencies close to the critical frequency, a sharp reduction in breakdown voltage is observed in Fig. 1, which is due to the accumulation of electrons in gap as explained in the third scenario. This regime can be referred to as the *transition regime*. For frequencies greater than the critical frequency, the breakdown voltage is almost constant and is approximately a factor of three lower than the DC

TABLE I. DC Breakdown voltages and predicted critical frequencies for various operating conditions.

Gas	γ_{se}	Gap (μm)	DC breakdown voltage (V)	Predicted critical frequency (GHz)
Nitrogen	0.1	19	130	6.3
Argon	0.05	0.5	33	1830 ^a
		2	110	382 ^a
		5	190	105
		10	177	24.6
Argon	0.09	15	172	10.6
		15	145	8.96
Argon	0.13	15	130	8.03

^aDue to FE dominated regime, the reduction of breakdown voltage at critical frequency is negligible.

breakdown voltage for this specific case. This regime, where the primary electron loss mechanism is diffusion (depending only on the operating pressure), is referred to as *diffusion controlled regime*. Finally, it is seen that at very high frequencies, breakdown voltage again starts increasing. This trend can be explained using the fact that the energy gained by electrons in the field decreases with increasing frequency.¹ This is a direct consequence of the decrease in electron oscillation amplitude as frequency increases. As a result, for the electrons to acquire sufficient energy to ionize neutrals and trigger an avalanche breakdown, the applied voltage has to be increased. This regime is referred to as the *inertia controlled regime*.

The first 10 ns time history of mean number densities of electrons and ions are shown in Fig. 2 for 6 and 6.5 GHz excitations. The mean number densities were obtained by time-averaging over half cycles. While for the same value of the applied voltage of 90 V, the number of electrons and ions continues to increase for 6.5 GHz, 200 MHz beyond the critical frequency, they decay for 6 GHz which is 300 MHz lower than the critical point. The difference in behavior between the 6 and 6.5 GHz is particularly striking considering that the frequency difference is only about 8% thereby clearly demonstrating the significance of the critical frequency (6.3 GHz) and the substantial decrease in breakdown voltage after the critical frequency.

The second case considered in this work used argon gas and nickel electrodes where φ was taken as 5.15 eV and β and γ_{se} were chosen as 55 and 0.05, respectively. Five different gap sizes of 0.5, 2, 5, 10, and 15 μm were chosen for comparison. It has been shown²⁴ that in a 500 nm gap, the almost only

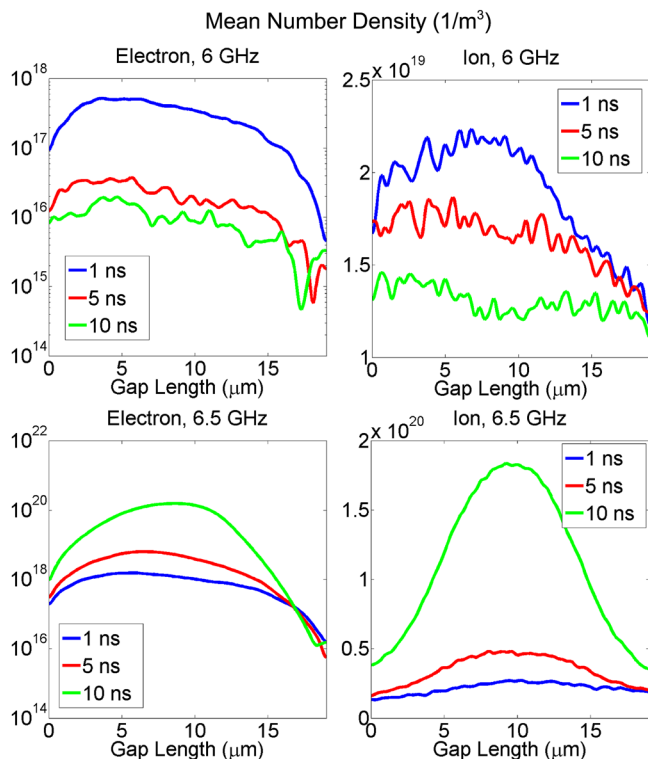


FIG. 2. Time variation of mean value of electrons and ions number densities in a 19 μm nitrogen gap with copper electrodes for 6 and 6.5 GHz excitations. $\varphi = 4.7$ eV, $\beta = 70$, and $\gamma_{se} = 0.1$.

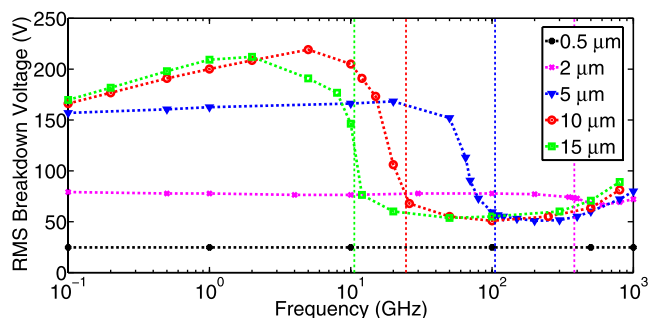


FIG. 3. Frequency response of breakdown voltages and the predicted critical frequency points in 0.5, 2, 5, 10, and 15 μm argon gaps with nickel electrodes. $\varphi = 5.15$ eV, $\beta = 55$, and $\gamma_{se} = 0.05$.

mechanism responsible for breakdown is FE. However, in 2 and 5 μm gaps, all three discharge mechanisms contribute. On increasing the gap size further to 10 and 15 μm , FE does not play any role with EII and SEE being the primary mechanisms responsible for breakdown. Therefore, the selected gap sizes allow us to understand frequency response of FE driven, transition and macroscale regimes of the modified Paschen curve for a time-varying field.

The simulation results for breakdown voltage of argon gap with nickel electrodes are summarized in Fig. 3. The critical frequency decreases rapidly with increasing gap length as can be seen in this figure. This is due to larger distance that electrons should pass to reach the electrodes and results in wider diffusion controlled regions in larger gaps. The decrease in breakdown voltage at the critical frequency is related to the contribution of FE to breakdown with a lower decrease indicating a higher FE contribution. Hence, although the predicted critical frequency for the 500 nm gap (Table I) is beyond the frequency range considered here, the reduction in the breakdown voltage will be negligible due to FE dominant regime.²⁴ For the same reason, the decrease in breakdown voltage for the 2 μm gap which occurs at around $f_{cr} = 382$ GHz is quite small. However, the variation of breakdown voltage for larger gaps which have low contribution from FE is large and strikingly similar to the results shown in Fig. 1 for nitrogen with copper electrodes. The width of the diffusion controlled regime also increases with the gap size.

For validating our simulations, frequency responses of a 15 μm argon gap for various values of γ_{se} were compared to experimental results²⁰ and are included in Fig. 4. The

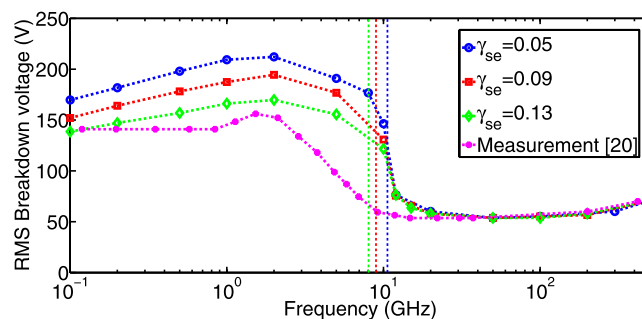


FIG. 4. Comparison of simulated and measured frequency response of breakdown voltages and the predicted critical frequency points in a 15 μm argon gap with nickel electrodes. $\varphi = 5.15$ eV, $\beta = 55$, and $\gamma_{se} = 0.05$, 0.09, and 0.13.

measurements were performed for DC to 1 MHz, 10^{-8} to 600 Torr, and 1 cm gap and were mapped to our high frequency atmospheric pressure microgap case by using $f \times d$ and $p \times d$ scaling factors. In general, good agreement is observed between measurement and simulation results for γ_{se} of 0.13. The main reason for the differences is that the presented experimental results in the boundary controlled regime are for $p \times d = 1$ Torr-cm, whereas, our simulations are for $p \times d = 1.14$ Torr-cm. Lack of information about several other experimental parameters is also affective. As expected, it is observed that changing γ_{se} varies the breakdown voltage only in the boundary controlled regime and has negligible effects on the diffusion and inertia controlled regimes in which, the ions do not have time to reach the electrodes and consequently there is no SEE, anymore.

According to Eq. (1), the breakdown voltage has to be known in advance to obtain the critical frequency which could be a potential disadvantage. However, since it was shown that the breakdown voltage does not change significantly in the boundary controlled regime, the DC breakdown voltage can be used instead of V_{rms} to obtain an approximate critical frequency. This would be a useful evaluation tool in finding failure regimes in high frequency micro/nanoelectronics. As described earlier, several well established theories exist to estimate the DC breakdown voltage for given operating conditions.^{9,10} In order to verify this, DC breakdown voltages and the corresponding estimation of the critical frequencies are tabulated in Table I for all cases. The estimated critical frequencies are in good agreement with those observed from PIC/MCC simulations summarized in Figs. 1 and 3.

In summary, frequency response of breakdown voltage of atmospheric pressure micro and nanoscale gaps was investigated using PIC/MCC simulations. It was shown that the frequency domain can be classified into four distinct breakdown regimes depending on the applied frequency. A critical frequency below which the breakdown is predominantly boundary controlled thereby resembling DC breakdown was observed. At around the critical frequency, the breakdown voltage displays a sharp decrease thereby transitioning to a regime where breakdown is diffusion controlled. At very high frequencies, the electrons no longer gain sufficient energy from the field thereby unable to participate in ionizing collisions. This leads to an increase in breakdown voltage at very high frequencies depending on the gap size. An approximate expression for predicting the critical frequency based on DC breakdown voltage was proposed and verified with the PIC/MCC simulations. This expression can be used to determine the range of safe operating voltages/frequencies for micro and nanoelectronic devices and circuits. The

results of this work will also aid in verification of analytical models to describe the frequency response of micro/nanoscale breakdown by extending the existing models for DC breakdown.

This paper is based upon work supported by the National Science Foundation under Grant No. 1202095.

- ¹Y. P. Raizer, V. I. Kisin, and J. E. Allen, *Gas Discharge Physics* (Springer, Berlin, 1991).
- ²F. Iza and J. Hopwood, *Plasma Sources Sci. Technol.* **14**(2), 397 (2005).
- ³T. Yokoyama, S. Hamada, S. Ibuka, K. Yasuoka, and S. Ishii, *J. Phys. D* **38**(11), 1684 (2005).
- ⁴C. H. Chen, J. A. Yeh, and P. J. Wang, *J. Micromech. Microeng.* **16**(7), 1366 (2006).
- ⁵B. N. Sismanoglu and J. Amorim, *Eur. Phys. J. Appl. Phys.* **41**(2), 165 (2008).
- ⁶R. H. Fowler and L. W. Nordheim, *Proc. R. Soc. London Ser. A* **119**(781), 173–181 (1928).
- ⁷P. Rumbach and D. B. Go, *J. Appl. Phys.* **112**(10), 103302 (2012).
- ⁸M. Radmilović-Radjenović, Š. Matejčik, M. Klas, and B. Radjenović, *J. Phys. D* **46**(1), 015302 (2013).
- ⁹D. B. Go and D. A. Pohlman, *J. Appl. Phys.* **107**(10), 103303 (2010).
- ¹⁰A. Venkatraman and A. A. Alexeenko, *Phys. Plasmas* **19**(12), 123515 (2012).
- ¹¹V. A. Lisovskiy, S. D. Yakovin, and V. D. Yegorenkov, *J. Phys. D* **33**(21), 2722 (2000).
- ¹²W. Zhang, T. S. Fisher, and S. V. Garimella, *J. Appl. Phys.* **96**(11), 6066–6072 (2004).
- ¹³Y. P. Raizer, M. N. Shneider, and N. A. Yatsenko, *Radio-Frequency Capacitive Discharges* (CRC Press, Boca Raton, 1995).
- ¹⁴J. L. Walsh, Y. T. Zhang, F. Iza, and M. G. Kong, *Appl. Phys. Lett.* **93**(22), 221505 (2008).
- ¹⁵V. Lisovskiy, J. P. Booth, K. Landry, D. Douai, V. Cassagne, and V. Yegorenkov, *EPL (Europhys. Lett.)* **80**(2), 25001 (2007).
- ¹⁶M. Radmilović-Radjenović and B. Radjenović, *Plasma Sources Sci. Technol.* **16**(2), 337 (2007).
- ¹⁷J. Rasch, D. Anderson, M. Lisak, V. E. Semenov, and J. Puech, *J. Phys. D* **42**(20), 205203 (2009).
- ¹⁸J. H. Booske, *Phys. Plasmas* **15**, 055502 (2008).
- ¹⁹S. C. Brown, *Proc. IRE* **39**(12), 1493–1501 (1951).
- ²⁰C. E. Muehe, Ac breakdown in gases, Technical report, DTIC Document, 1965.
- ²¹D. Anderson, U. Jordon, M. Lisak, T. Olsson, and M. Ahlander, *IEEE Trans. Microwave Theory Tech.* **47**(12), 2547–2556 (1999).
- ²²J. Rasch, D. Anderson, M. Lisak, V. E. Semenov, and J. Puech, *J. Phys. D* **42**(5), 055210 (2009).
- ²³T. Pinheiro-Ortega, J. Monge, S. Marini, J. Sanz, E. Sorolla, M. Mattes, C. Vicente, J. Gil, V. E. Boria, and B. Gimeno, *IEEE Microw. Wirel. Compon. Lett.* **20**(4), 214–216 (2010).
- ²⁴A. Semnani, A. Venkatraman, A. A. Alexeenko, and D. Peroulis, *Appl. Phys. Lett.* **102**, 174102 (2013).
- ²⁵C. K. Birdsall, *IEEE Trans. Plasma Sci.* **19**(2), 65–85 (1991).
- ²⁶V. Vahedi, G. DiPeso, C. K. Birdsall, M. A. Lieberman, and T. D. Rognlien, *Plasma Sources Sci. Technol.* **2**(4), 261 (1993).
- ²⁷J. Reece Roth, *Industrial Plasma Engineering: Volume I-Principles, Section 12.5.2* (IOP, Bristol and Philadelphia, 1995).
- ²⁸A. Venkatraman, A. Garg, D. Peroulis, and A. A. Alexeenko, *Appl. Phys. Lett.* **100**(8), 083503 (2012).